Indexes for performance evaluation of cameras applied to dynamic measurements

Giorgio Busca [a,*], Giulia Ghislanzoni [b], Emanuele Zappa [a]

[a] Politecnico di Milano, Dipartimento di Meccanica, Via La Masa 1, 20156 Milan, Italy
[b] CEMB S.p.A., Via Risorgimento 9, 23826 Mandello del Lario (Lc), Italy

Article history:
Received 1 August 2013
Received in revised form 10 January 2014
Accepted 4 February 2014
Available online 11 February 2014

1. Introduction

Imaging devices have been intensively studied as displacement transducers in the last 20 years. There are many advantages in using such devices. First, the measurement is remote, contactless and dense, which means that it is possible to perform a multipoint measurement with one single camera, where each pixel of the sensor matrix is like a single transducer. Secondly, the measurement set up is really easy and flexible to manage, since only one camera, some targets and a personal computer are needed [1–3].

The use of imaging devices as displacement transducers was firstly proposed in almost-static applications, where the acquired object moves slowly with respect the acquisition parameters of the camera and therefore the target displacement during the exposure time can be neglected. Thanks to technology improvements, the applications of vision-based measurement to dynamic applications have been increasing in the last 10 years [4–7]. The available image resolutions and the high grabbing frequencies allow

* Corresponding author. Tel.: +39 23998445.
E-mail address: giorgio.busca@polimi.it (G. Busca).

to acquire high-speed moving object with a good scaling factor and to perform dynamic analysis of vibrating items. Currently, a basic imaging device can easily acquires 1 Megapixel images with a 25 fps grabbing frequency, which means that it is possible to perform a dynamic analysis up to 12.5 Hz at full resolution, but there are also top level cameras able to acquire 2–3 Megapixel images with more than 2 kHz grabbing frequency. One of the most common application of vision-based techniques to dynamic analysis is the structural health monitoring (SHM), where vision-based measurements are used to identify displacements and vibrations of whole civil structures and their components [8–12].

Since imaging devices are used as transducers, some assessments about their measurement uncertainty should be done. Uncertainty of vision-based measurement is affected by several factors which define the image quality, such as image resolution, scaling factor (px/mm ratio or vice versa), focusing quality, lighting conditions, and image contrast, aberration. Their effects on measurement uncertainty are not easily quantifiable. For example, Cantatore et al. [13] and Shimizu and Okutomi [14] demonstrated that a moderate blurring may reduce the measurement uncertainty. Moreover, these image properties might be obtained adjusting several camera acquisition parameters, which could depend on each other. For example, different combinations of exposure time and diaphragm aperture could produce the same image luminance or contrast. However, this might be achieved with different side effects: reducing the diaphragm aperture decreases the image luminance, but it increases the depth of view; on the other hand, reducing the exposure time may obtain the same results on the image luminance, together with a decreasing of the amount of noise.

Since the quantification of the measurement uncertainty depends on several parameters, it is comprehensible how could be useful the definition of some synthetic indexes, in order to define the image quality and consequently the measurement uncertainty in static and dynamic conditions. The quantification of the measurement uncertainty when imaging devices are used in dynamic conditions becomes more challenging and important, since in this case other factors, in addition to those listed before, are fundamental to define the measurement performance, such as the camera-object relative motion in terms of instantaneous velocity and acceleration. The good displacement estimation will indeed depend on the dynamic camera parameters, such as grabbing frequency, but, most of all, the exposure time that must be settled to a proper value in order to avoid motion blurring.

In this work some indexes, based on exposure time and Spatial Frequency Response function (SFR), will be proposed and qualified. The indexes proposed in this work are suitable to define the measurement uncertainty both in static and dynamic condition and it will be showed how their behavior is linked to the measurement uncertainty. The results proving this statement are obtained by several tests, where a target is moved with a harmonic law in controlled conditions (varying its frequency and amplitude) and fixing different acquisition characteristics in terms of lighting conditions, diaphragm aperture, exposure time, etc.

In the next section, some concepts about the estimation of the image quality by means of the Spatial Frequency Response (SFR) will be fixed. The results performed in static conditions are the basic point to start the analysis in dynamic conditions. Then, in Section 3 the dynamic qualification are provided and in Sections 3.4-3.6 three indexes for the image quality estimation in the case of dynamic acquisition conditions will be proposed and applied. The advantages and the limits of these indexes will be shown and it will be proven how they can be applied to uncertainty measurement qualification.

2. Static qualification

The performance of cameras applied to dynamic measurement depends on several parameters; some of them can be evaluated in static condition, such as focus, lighting conditions, lens distortions, and image contrast. All these parameters work together to define the image quality. For these reasons, before performing an analysis focused on the dynamic performance, this section deals with some considerations about the imaging device behavior for acquisition in static condition. Some results about the image quality estimation will be presented with attention to image focus and diaphragm opening, which are parameters strictly linked to static acquisition, but also testing the influence of the shutter time value, which is linked both to static and dynamic acquisition. Shutter value, indeed, defines the amount of light impacting on the sensor but, most of all, the grabbing velocity of the acquired frames of the moving object. In this way, it will be possible to divide the contribution of static parameters from those of the dynamic parameters in the image quality definition, under dynamic grabbing condition.

2.1. SFR function

In static condition the image quality rendered by an imaging system can be evaluated by the Spatial Frequency Response (SFR), defined in ISO 12233 [15]. The SFR has been widely used to characterize the spatial frequency response of many kinds of imaging systems. It is defined as the modulus of the Optical Transfer Function (OTF), which is the Fourier Transform of the impulse response of the system [16]. It defines the ability of an optical system to resolve a contrast at a given resolution (or spatial frequency). Traditional methods for SFR measurements were initially designed for analog cameras [17–19].

However, when digital cameras are considered, these techniques can give misleading SFR results, because the sampling of digital devices is not properly considered. Additionally, SFR results estimated with the mentioned traditional methods can depend on the chosen technique (sine target or bar target utilization, slit or knife-edge technique). The ISO 12233 methodology has been established in order to provide a fast SFR measurement method based on one image only. In such a standardized way, the SFR

data (from various digital input devices) may be easily and correctly compared.

In this paper the slanted-edge method proposed in ISO 12233 is used [15,16,20,21]. The technique consists in imaging an edge slightly tilted with respect to the rows (or the columns) of the detector, as shown in Fig. 1. Therefore, a nearly vertical edge allows obtaining the horizontal Spatial Frequency Response (SFR) of the imaging system, while a nearly horizontal one can be used to estimate the vertical SFR. The detailed description of the procedure for the estimation of SFR is out of the scope of this work and can be found in ISO 12233; the basic steps for SFR computation procedure are summarized in the following. If the edge in nearly vertical, a region of interest (ROI) containing the edge must be selected and each row of the ROI is an estimate of the camera edge spread function (ESF) along the horizontal direction. Each of these edge spread functions is differentiated to form its discrete line spread function (LSF). The next step is the super-sampling and averaging of all the edge spread functions to form an average estimation ESF that is more finely sampled than each original ESF. The averaged, super-sampled ESF is then processed by a point-spread function reconstruction algorithm or by application of a Fourier transform-based method. The obtained SFR characterizes the transfer of spatial frequencies related to the observed objects.

The aim of this work is to apply the SFR estimation to define some quality indexes of the camera performance in case of dynamic target conditions. First, this section shows some results about the SFR estimation in case of static grabbing condition, in order to fix some concepts useful to the comprehension of this work. The camera used for the tests is a Marlin F131B camera, equipped with 16 mm and 25 mm focal length lens (to explore the variation of the results with this parameter). The static target used to qualify the device is the one reported in ISO 12233 and shown in Fig. 1a. The SFR function is evaluated in different conditions such as focal length, image focus, diaphragm opening and exposure time, as it will be shown in the following.

As known from literature, image defocus affects camera performance in terms of SFR [22]. Fig. 2 shows two SFR curves obtained with the same acquisition hardware and target, but with two focusing conditions. The SE value, shown in the figure legend, is the sampling efficiency, which is estimated by the Rayleigh criterion as the ratio between the sampling resolution (cycle/pixel), where the SFR is equal to 0.1 (expressed in terms of cycle/pixel ratio) and the half sampling resolution 0.5 cycle/pixel (Nyquist spatial resolution) [15]. It is clear how the defocused image gives the worst results, for both the SE value and the 0.5 SFR point (SFR_50), i.e. the spatial frequency where SFR assumes the value 0.5: the modulus decays very fast as the spatial frequency increases, consequently the SFR_50 is set in correspondence of 0.1 cycle/pixel ratio.

The influence of the diaphragm is more difficult to define with respect to the focus condition. The diaphragm opening is related to two well-known distortion effects, which concern vision devices: lens aberration and diffraction. When the diaphragm is open, the lens aberration is evident, whereas the diffraction effect is lower. A compromise condition should therefore be found. However, this condition depends on the hardware characteristics. As for the specific hardware configuration used in this work, Fig. 3 shows the SFR curves obtained by different combinations of shutter and diaphragm values in order to obtain the same image contrast (a difference between black and white of at least 200 grey levels). For example, the analyzed combinations show that the optimum (maximum SFR modulus) for the 25 mm lens (Fig. 3(a)) seems to be at the 5.6 f/stop value (SE = 100%), but good results are also obtained for f/stop 2.8 and f/stop 4. Fig. 3(b) shows the same analysis with a 16 mm focal length optic. The results state that for the experimental conditions considered in this work, the best performances are obtained with the minimum diaphragm aperture (5.6 f/stop).

As previously described, Fig. 3a and b shows the combined effect of reducing the diaphragm aperture (i.e. increasing the f/stop value) and contemporarily increasing the exposure time (shutter) to ensure a constant contrast (200 grey levels) between dark and bright image regions. On the contrary, Fig. 4 shows the SFR curves obtained changing only one of these parameters at a time, in order to analyze the effect of the diaphragm and shutter value

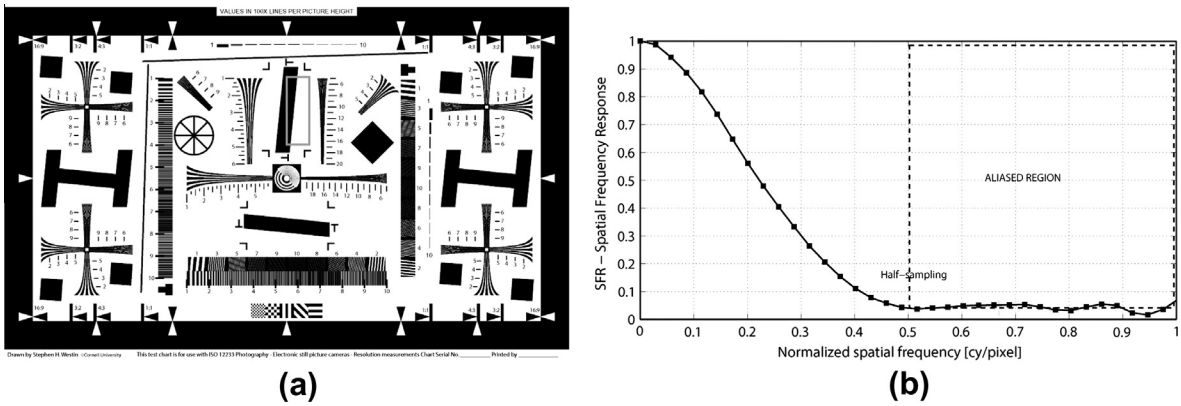

Fig. 1. (a) Target used for the tests and proposed by ISO 12233. The red square specifies the portion used to evaluate the SFR curve and (b) the response of a digital sensor to a slanted-edge input.

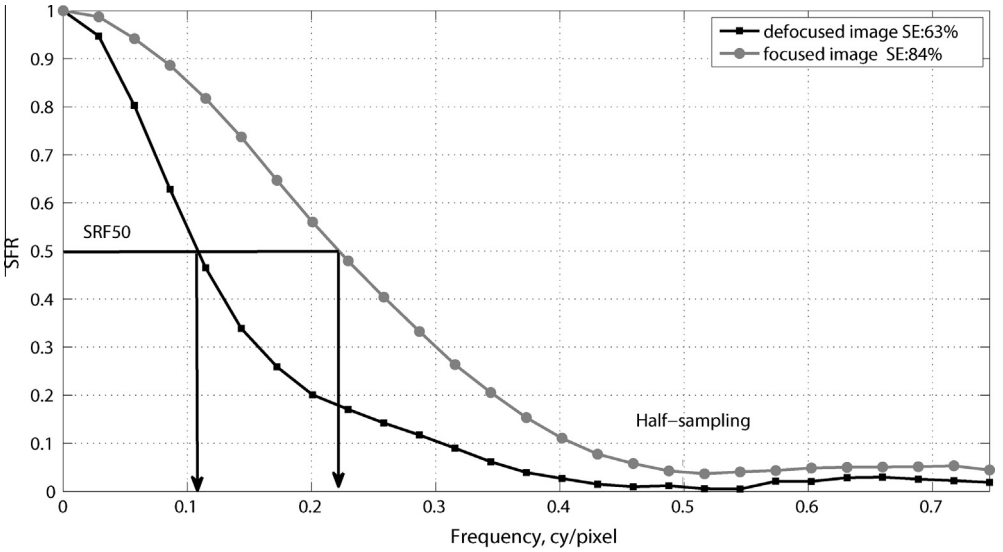

Fig. 2. SFR of focused and defocused images grabbed by a camera equipping a 16 mm focal length lens, with a 2.8 diaphragm and a 20 ms shutter.

separately. In these tests, the light intensity was tuned to ensure again a contrast of 200 grey levels between dark and bright regions of the image.

In Fig. 4 the SFR curve, referred to diaphragm 2 and shutter 16 ms, and one, referred to diaphragm 2.8 and shutter 32 ms (the light has half passage area and the shutter is two times longer), have the same SE value equal to 80%. However, the SFR curve with diaphragm 2.8 shows higher values for cycle/pixel range between 0 and 0.45, which means that the SFR curve quality mainly depends on the f/stop value. Moreover, Fig. 4 shows that SFR curves assume larger values with lower exposure times (which corresponds to higher illumination intensity to ensure a constant contrast level) when f/stop value is fixed. This last result is reasonable because, reducing the exposure time, the noise level of the image tends to reduce accordingly.

In conclusion, these tests state that the image quality increases in static conditions as the f/stop is high, the shutter time is low and the image is well focused. The results obtained in terms of SFR curves are known in literature, but they are necessary to introduce the next section about the dynamic qualification of cameras, since it is based on the application of SFR curves.

3. Dynamic qualification

The previous section briefly describes in terms SFR curve the conditions that affect the image quality, when the target is static with respect to the camera. This section describes the dynamic tests performed to evaluate the performances of a camera sensor acquiring a target moving with a harmonic law. The tests aim to find a connection between the target sinusoidal displacement parameters (i.e. the amplitude and the frequency of the motion), the camera acquisition parameters and the measurement uncertainty. The camera acquisition parameters, which are considered significant, are the image acquisition frequency and the shutter value, which are the variables the dynamic measurement depends on, plus those which can affect the static measurement: for example the resolution quality, expressed in terms of mm/px ratio, the image focus or the lens distortions.

3.1. Measurement setup

The experimental tests are done in controlled conditions in order to perform a meaningful dynamic performance qualification, trying to keep constant all the uncertainty sources and the camera-target relative motion. A proper measurement setup is designed to guarantee the control on the tests, as shown in Fig. 5. A planar black and white target is placed on a rigid aluminum support to prevent appreciable deformation of the pattern itself during the tests. The target displacement is imposed by an electrodynamic actuator, equipped with a closed loop control system to guarantee stability and accuracy to the imposed harmonic displacement. A laser doppler vibrometer, model Polytec Scanning Vibrometer PSV300 (2.56 μm resolution) is also used as a reference for the target displacement and velocity measurement, along the vertical direction.

The moving target acquisition is made by a Marlyn F131B camera, equipped with a 16 mm focal length lens, a 1280×1024 pixel CMOS sensor (cell size $6.7\ \mu m \times 6.7\ \mu m$), maximum acquisition frequency 25 fps, settable exposure time with 20 μs resolution. The camera is placed in front of the target in order to have the optical axis normal to the planar target surface, which is necessary to measure only the vertical displacement. Finally, the lighting test conditions are guaranteed by two led lights placed near the camera, with their pointing direction at 45° with respect to the camera optical axis.

Thanks to a unique trigger signal for interferometer and camera, the two measurements are synchronized. The maximum delay between the trigger signal and the beginning of the exposure time is negligible in most of the commercial cameras and therefore this uncertainty source can often be neglected for the application in mechanical

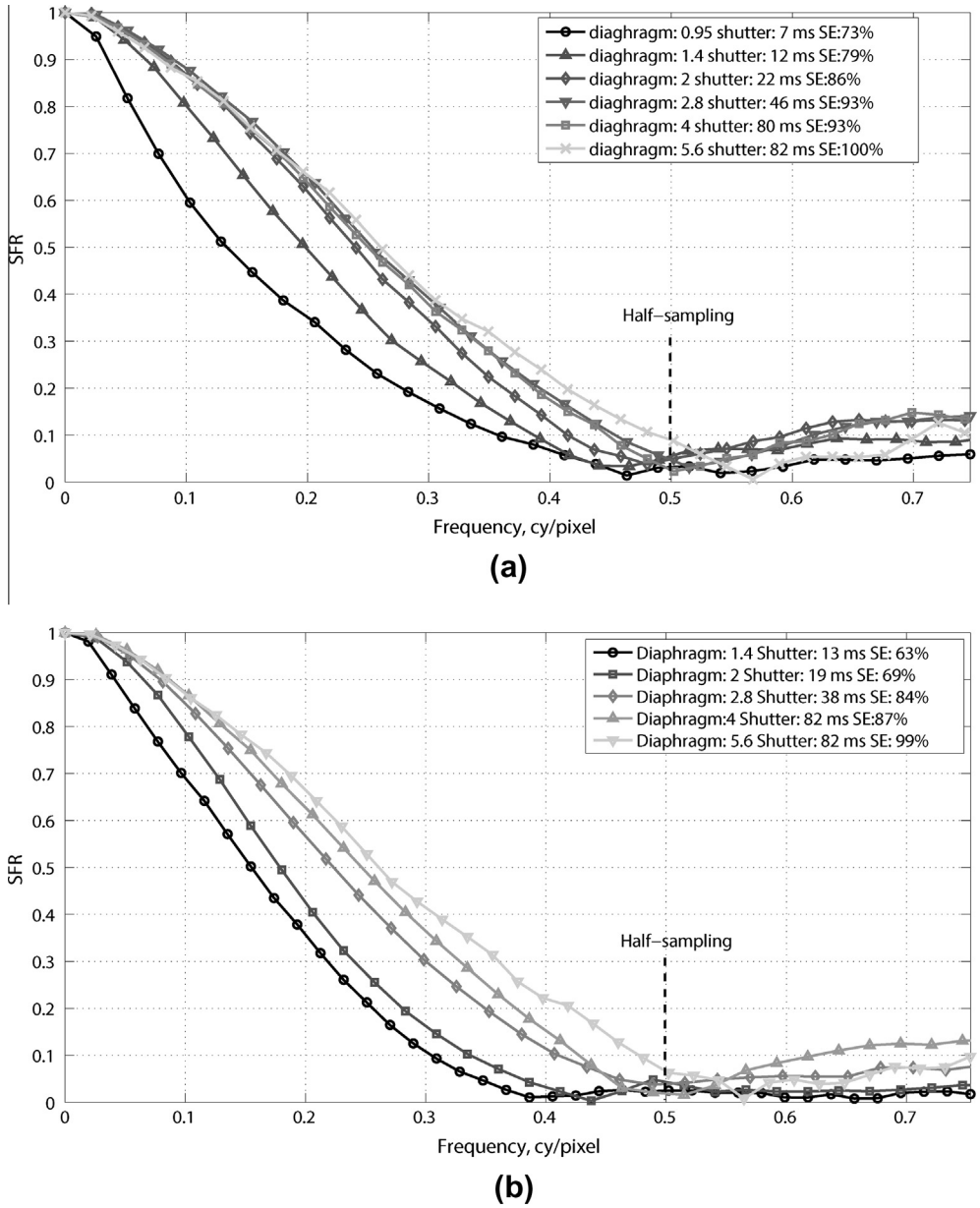

Fig. 3. SFR curves for different values of diaphragm and shutter: (a) 25 mm focal length optics and (b) 16 mm focal length optics.

vibration measurements. For instance, the delay of a F131B Marlin camera used in this work is below 25 ns.

The above measurement setup is considered suitable to ensure a complete control on the tests, which need to be performed with several target displacement characteristics in terms of amplitude, frequency and, at the same time, several acquisition parameters in terms of grabbing frequency, exposure time and lighting conditions.

3.2. Dynamic test conditions

As previously stated, the test parameters may be chosen at two levels:

- *Motion parameters*: amplitude and frequency displacement.
- *Acquisition parameters*: grabbing frequency, shutter value (i.e. exposure time) and lighting levels.

The parameters values are chosen in order to have the most complete description of the dynamic camera performance, paying attention to the instrumentation practical limits. The target is moved according to mono-harmonic displacements in order to study simple case, which can be easily verified and repeated.

It should be underlined that, almost mono-harmonic displacements are quite common in the practice of mechanics, since vibration components at higher frequen-

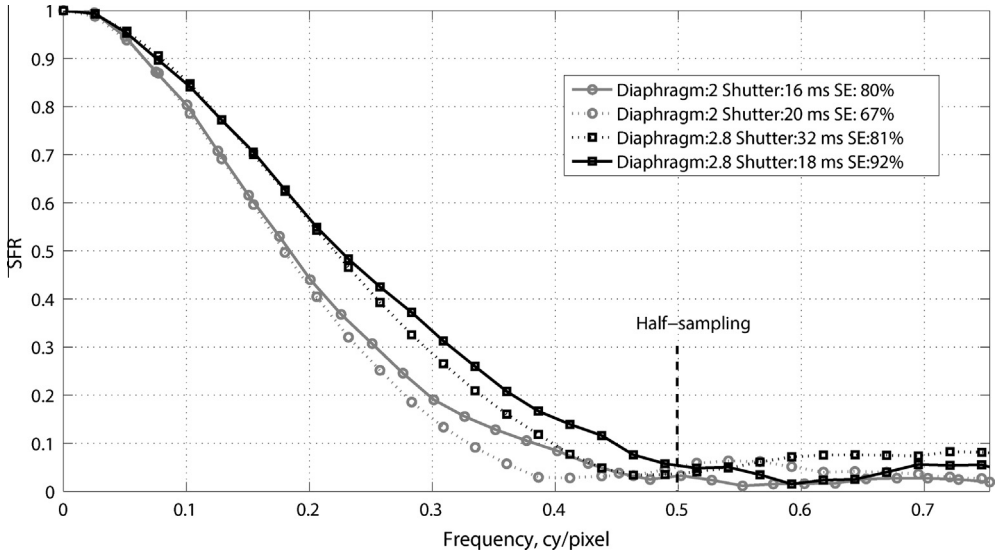

Fig. 4. SFR curves for two diaphragm values and two shutter levels (16 mm focal length optics).

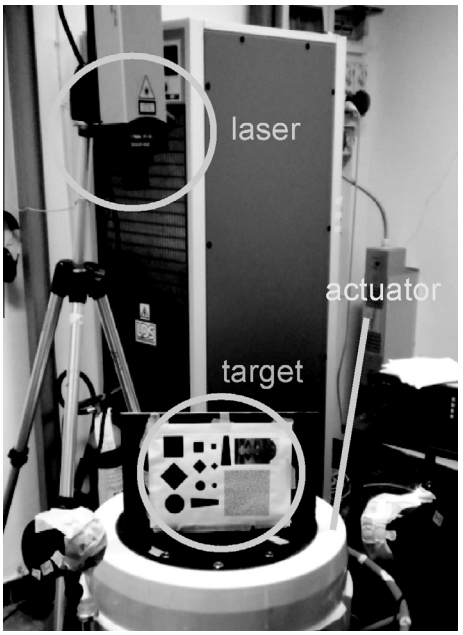

Fig. 5. Measurement setup.

cies are usually linked to smaller displacements and therefore can often be neglected if compared to the low frequency one. In the case of acceleration measurements high frequency are of course highlighted by ω^2 term but, since the camera measures displacements, the assumption of mono-harmonic signal is often acceptable in practice. Moreover, the acquisition frequency of medium price cameras are often limited to a few tenth of Hertz if a resolution of at least 1 Megapixel is needed, and therefore cameras have sometimes to be used in controlled aliasing condition, which is a solution effectively applicable if almost mono-harmonic vibration has to be measured.

The test are designed combining four frequency levels (5 Hz, 10 Hz, 15 Hz and 20 Hz) with five displacement amplitude levels (0.5 mm, 1.5 mm, 3 mm, 5 mm and 7 mm) for a total of 20 motion conditions. For each of these conditions, tests with 5 different exposure shutter time (4 ms, 5 ms, 10 ms, 15 ms and 20 ms) were done. Since there is a data transmission restriction from the camera to the PC, the imaging device used for the tests has a maximum grabbing frequency of 25 Hz in full resolution condition (1280 $\times$ 1024 px). In order to perform the tests with a target vibrating at frequencies higher than 12.5 Hz, the sampling theorem would require an out of range grabbing frequency. Therefore, all the tests with a frequency displacement greater than half the maximum grabbing frequency (25 Hz) are acquired in controlled aliasing condition.

All the images are grabbed with a nominal scaling factor of 3 pixel/mm and the 2D-camera calibration is done before each test sessions to estimate the actual scaling factor. Moreover, a f/4 diaphragm value is chosen as good compromise between the SFR curve and the image luminance. All the tests are performed with a 16 mm focal length lens. Table 1 summarizes the tests conditions in terms of frequency displacement, amplitude displacement (both in millimetres and in pixels) and camera parameters: all the possible combinations define one hundred different test conditions.

Once the videos of the moving target (see Fig. 5) are acquired, each frame is analyzed by a pattern matching technique to detect the position of the object inside the camera field of view, in order to estimate its displacement. Among the several image processing techniques this is one of the most used for displacement estimation, since it requires simple algorithms and guarantees good measurement uncertainty [2,3]. In the next section, some indexes will be proposed to qualify the measurement performance of the pattern matching technique applied to the several test conditions of Table 1.

Table 1
Levels of the test parameters (frequency and amplitude displacement, camera shutter value) for a total of 100 combinations.

Frequency (Hz)	Amplitude (mm)	Amplitude (px)	Shutter (ms)
5	0.5	1.5	4
10	1.5	4.5	5
15	3	9	10
20	5	15	15
	7	21	20

3.3. Discrepancies

One of the simplest way to compare the displacement imposed by the actuator with the one estimated by the camera is the discrepancy evaluation between these two quantities. The value of the displacement measured by the laser doppler can be considered as reference, since this transducer has an uncertainty negligible with respect to the pattern matching technique.

Before doing the comparison, it is useful to fix some concept about the exposure time. Since the exposure time is non-zero in dynamic conditions a problem might arise: which is the exact instant of time to whom the image can be apportioned to? We analyzed the effect of the exposure time comparing the time history measured by the interferometer with the one acquired by the camera, and we found that minimum discrepancy is obtained when the positions measured by the camera are considered related to an instant of time in the middle of the exposure time. This result is valid for all the considered conditions (different exposure times and target motion parameters) and we concluded that the effect of the exposure time in dynamic measurement is to create a constant time delay depending on the exposure time value. Due to this reason, for all the results shown in the following, the delay due to the exposure time will be compensated.

In Fig. 6(a) the comparison in time domain between camera and laser is shown in the case of a test with f = 15 Hz, amp = 5 mm, shutter = 10 ms, and the time shift equal to the half of the exposure time was compensated; thanks to this operation, time shift between camera and laser is no longer present. Since the tests were done in controlled aliasing conditions, in order to compare the laser and the camera data it is necessary to down sample the laser data. In Fig. 6 the camera data and down sampled laser data are shown together with the point-by-point difference between the camera and laser signal.

In Fig. 6(b) it can be seen that the over/under-estimation of the camera has a periodic trend with period equal to the period of the signal (Fig. 6(a)).

Since the discrepancy is a function of the instantaneous position, it is possible to assess the uncertainty on the amplitude estimation, whereas the uncertainty on the instantaneous position depends on the motion condition (i.e. it is not constant in time). It is of course possible to express the maximum uncertainty on instantaneous position (0.15 mm in the example of Fig. 6(b)) but in the case of mono-harmonic motion law, the amplitude information is in our opinion more significant.

The same point-by-point comparison were done for different combinations of shutter time, motion amplitude and

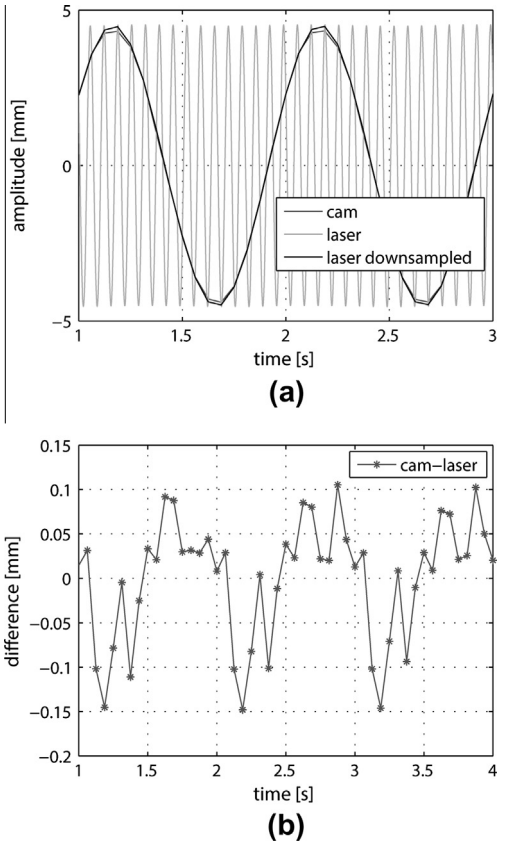

Fig. 6. Test f = 15 Hz, amp = 5 mm, shutter = 10 ms (a) time histories of the camera and laser downsampled at the same frequency of the camera and (b) difference between camera and laser data.

motion frequency values and very similar behavior is found in all the cases.

Thanks to the comments above, from now on the analysis will be focused on amplitude estimation uncertainty.

The discrepancy between the displacement amplitude estimated by the laser doppler and the one estimated by the pattern matching technique is evaluated for each of the twenty motion configurations described in Section 3.2 and for each of the five considered shutter times. The total of the tests condition combinations are one hundred and are repeated two times in order to verify the test repeatability. Once the displacement amplitude is estimated in the frequency domain by Fourier transform, the percentage discrepancy is calculated as follows:

$$\varepsilon = \frac{A^L - A^C}{A^L} * 100, \tag{1}$$

where A^L is the displacement amplitude measured by the doppler laser and A^C is the estimated one by means of the pattern-matching algorithm. The discrepancy estimation is performed in the frequency domain on a integer number of cycles of the signal in order to avoid the leakage error and other advantages: the dynamic analysis usually works with frequency component amplitudes, the harmonic amplitude is a synthetic index, and the discrepancy

evaluation in correspondence of one harmonic component may filter the negative effect of the noise spreads on the others frequencies.

Fig. 7 shows the results of the discrepancies obtained with a shutter time fixed at 4 ms. The distribution of the data as a function of the harmonic frequency reveals that there is not any evident trend of the discrepancy, with the considered shutter time and motion parameters. The discrepancy values are lower than 5% for almost all the cases.

However, when the exposure time is longer, for example 20 ms, the discrepancies show an increasing trend as the frequency of the motion increase, as shown in Fig. 8. This increasing trend is almost negligible with displacement amplitude of 1.5 px, whereas it becomes more and more relevant for the higher amplitudes.

The above results seem to point out that the discrepancy increases as both the exposure time and the motion amplitude increase. The question seems to be very simple from a mechanical point of view, but the uncertainty quantification of the detectable displacement is a central task for the application of cameras as displacement transducers. For this reason, the next sections will be focused on the definition of non-dimensional indexes useful to predict the uncertainty level as a function of the motion and acquired parameters.

3.4. E2PR

In the previous section, the results show that measurement error depends on the exposure time and the frequency of the object motion. Now it is proposed to merge these two variables in one single index, which could be named exposure to period ratio (E2PR), and it is defined as:

$$\mathrm{E2PR} = \frac{t_{\mathrm{exp}}}{T_{\mathrm{d}}}, \tag{2}$$

where t_{exp} is the exposure time and T_{d} is the period of the target harmonic displacement. An E2PR value of 0.15 represents for example an exposure corresponding to 15% of the target motion period. This index is defined on a displacement law that should be almost mono-harmonic.

Fig. 9 shows the discrepancy values measured for all the tests listed in Table 1 and plotted as a function of the E2PR value. The data distribution identifies two separate situations. When E2PR is below the value 0.1, the discrepancies do not show any evident trend and the data are uniformly

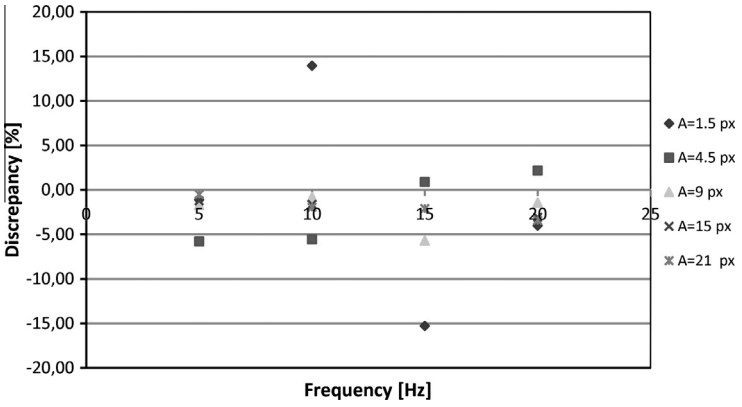

Fig. 7. Discrepancy vs. signal frequency with shutter time 4 ms.

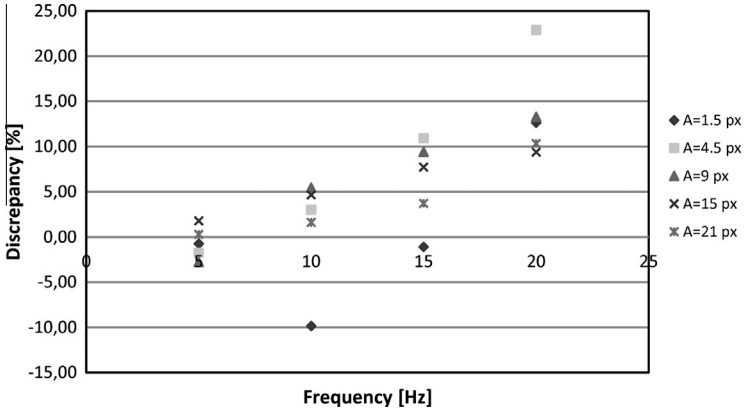

Fig. 8. Discrepancy vs. signal frequency with shutter time 20 ms.

distributed between the minimum value −0.5 px and the maximum value 0.5 px. In this condition, the measurement could be considered static and the discrepancy values are only due to the uncertainty of the pattern matching technique. On the other hand, when the E2PR value is larger than 0.1, the discrepancy distribution shows an increasing trend with a slope that becomes larger as the target amplitude increases.

Since the discrepancy ε is defined by Eq. (1) as the amplitude measured by the laser minus the amplitude measured by the camera, the positive discrepancy values shown in Fig. 9 mean the camera tends to underestimate the motion amplitude and this becomes more evident when the E2PR and the target vibration amplitude increase. This statement can be explained looking at Fig. 10, where the grey sinusoid represents the vertical displacement of a target as function of time. If the exposure time is non-negligible, when the target moves from point A to point B along the grey line, the camera does not detect the exact object position, but a sort of mean value of all the positions occupied by the target during the transition from A to B. Then, the amplitude is underestimated.

It must be noticed that the same conclusions were obtained from the analysis of different ROI of the target image, which means the camera performances do not depend on the chosen pattern.

3.5. Dynamic SFR

The previous section shows how the exposure time is a key parameter for the correct acquisition of moving targets. When the exposure time is set to a value that ensures E2PR $\leqslant$ 0.1, the test is performed in an almost-static condition and the estimated amplitude is not affected by any appreciable bias. In this section it is described a further analysis on the detection of moving targets based on the evaluation of the SFR curves in correspondence of each frame of the moving object videos. The aim is to find an index to quantify the motion effect on the image quality (and therefore on the accuracy of the detected target position)

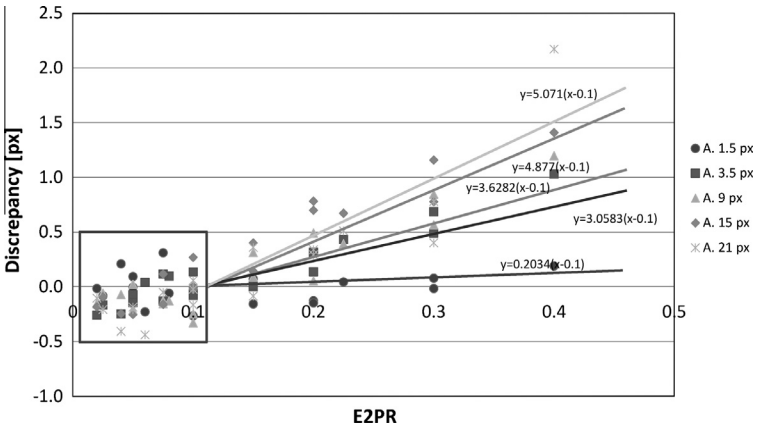

Fig. 9. Discrepancy vs. E2PR.

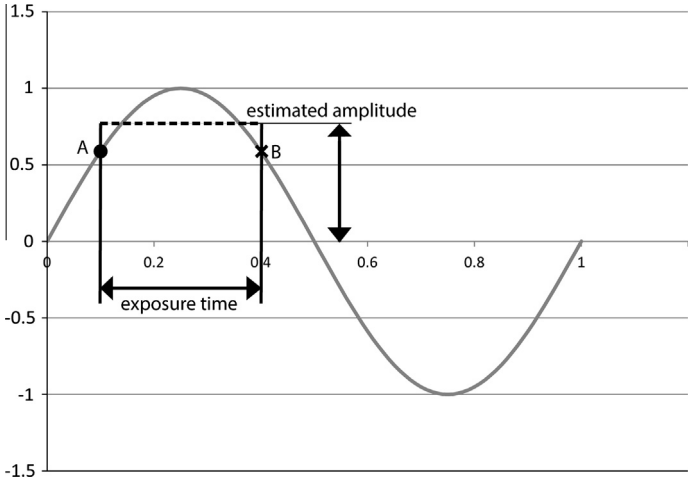

Fig. 10. Amplitude estimation when shutter value is too high.

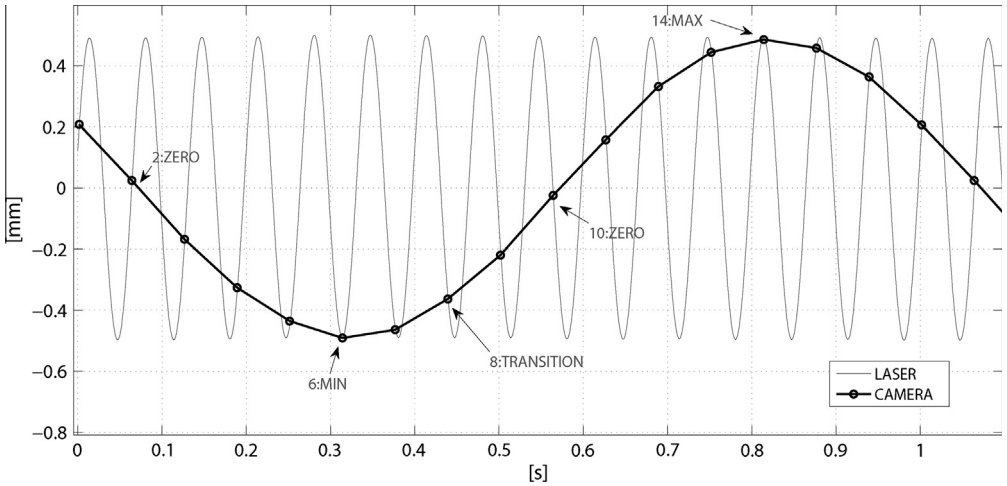

Fig. 11. Data measured in tests conditions A: amplitude 0.5 mm, frequency 15 Hz, shutter 4 ms, camera in controlled aliasing.

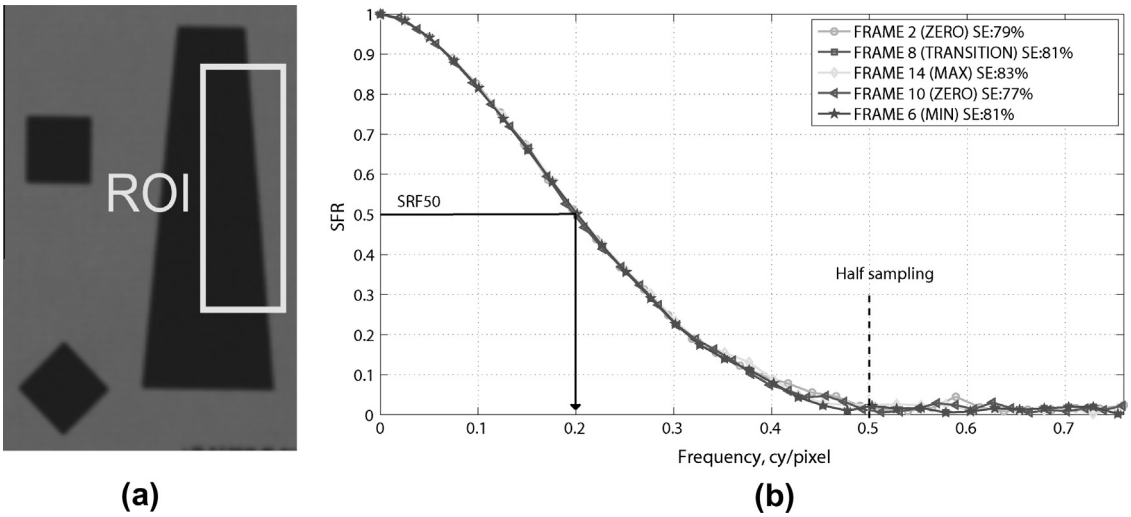

Fig. 12. (a) Sample image of the ROI used for SFR estimation and (b) correspondent SFR functions in test condition A.

that does not require any a priori knowledge of the target motion parameters, but only based on the analysis of the acquired images.

The proposed index is based on this observation: when the instantaneous velocity of the target grows, the motion blurring effect, registered by the camera during the exposure time, becomes more evident. The analysis with the E2PR parameters shown that, as the motion effect increases, the uncertainty of the measured motion becomes more relevant. It is possible to infer that the motion effect worsen the measurement accuracy, as it is reasonable to be expected. Therefore, an index capable to express quantitatively the motion effect on the measurement uncertainty would be very desirable. It is proposed here to use the variability of the SFR values, evaluated for different frames acquired during the motion of the target, as an index of the motion effect perceived by the camera. This index will be named dynamic SFR (SFR_σ).

In the next sections, two sample test conditions will be analyzed to describe the principle of the proposed procedure to estimate the SFR_σ index; whereas, in the second part, the dynamic SFR analysis will be applied to all the tests previously analyzed with the E2PR parameter and summarized in Table 1.

3.5.1. Dynamic SFR computation

It was shown in Section 2 that the SFR function is affected by the focusing of the image; moreover, the motion effect was also shown to have a blurring-like effect that leads to a spread of SFR functions associated to different frames of the movie of a moving target (Fig. 13). The basic idea of the SFR_σ index proposed here is to quantify the spread of the SFR function among the frames and use this as an index of the motion effect on the acquired images quality.

To implement the procedure the target should include a nearly vertical edge (tilted of 5°, as recommended in ISO 12233) for the SFR_σ estimation. Since SFR function was designed to analyze the response of the optics to an ideal edge input, it is assumed in SFR computation that the line spread function (LSF) is a smooth bell-shaped function (similar to a Gaussian function). Due to this assumption in the SFR_σ estimation procedure proposed in this work, a slanted edge nearly parallel to the motion direction is considered (region R2 in Fig. 14), because, if the region R1 is used, the obtained LSF functions would not be smooth and bell-shaped due to a too strong motion blurring effect, not allowing to obtain a meaningful SFR estimation.

In order to explain the estimation technique for the proposed SFR_σ index, two sample tests – described below – will be used. For each of the two tests, the analysis is applied to a portion of the video: the frames in correspondence of one period of the displacement acquired by the camera in aliasing condition. Among these frames, some of them considered significant for the analysis are chosen for this example: the maximum displacement, the minimum, the zeroes and the transitions (mid points between the limits and the zeroes). Fig. 11 shows the displacement of the target measured by the laser (grey signal) and the displacement detected by the camera (black signal) in the case of a test with 0.5 mm amplitude and 15 Hz frequency with a 16 Hz grabbing frequency and shutter value 4 ms. These test conditions will be referred to as "test conditions A" in the following. Obviously, the two signals have different frequencies because the acquisition is performed in controlled aliasing condition. The arrows point to the frames chosen for the analysis. The obtained SFR curves (estimated analyzing the region of interest (ROI) highlighted in Fig. 12a) are shown in Fig. 12b), one for each of the selected frames and it can be seen that they are well superimposed. Even the SFR-50 and SE values are almost the same for all the curves.

As can be seen in Fig. 12 the SFR curves do not show any evident change among the frames. This evidence shows that the motion effect is almost negligible in this case. On the contrary, if a different test condition is considered (referred to as "test condition B", see Fig. 13), with target displacement of 5 mm, motion frequency of 20 Hz and shutter time of 15 ms, a larger spread of the SFR curves for different frames is obtained (see Fig. 14). In this case, the MTF curves are evidently scattered and the SRF_50 values show a significant variation among the curves.

The SFR curves behavior can be explained by a wrong selection of the acquisition parameters, especially the exposure time. Indeed, analyzing the frames selected in Fig. 11 (test condition A), it is possible to see in Fig. 15 that they are perfectly clear and no motion blurring is present, but the frames selected in Fig. 13 (test condition B) are fuzzy, especially in correspondence of the points where the target has the maximum velocity (frames "zero" and "transition" in Fig. 15). Since the SFR curves' spreading is correlated to the quality of the dynamic acquisition, the standard deviation of these curves can be used to define a new index, as shown in Section 3.5.2.

3.5.2. Dynamic SFR applied to full test movies

As explained in the previous section, the SFR curves dispersion can be related to the dynamic measurement performance of an imaging device. This index is based on the standard deviation of the SFR curves measured in correspondence of each frame of a video, grabbing a moving target, which is expressed by the following function:

$$\text{SFR\_}\sigma = \sqrt{\frac{1}{N}\sum_{i=1}^{N}\sigma_i^2}\ (\text{cycle/pixel}), \tag{3}$$

where σ_i is standard deviation among the curves (each curve corresponding to a frame) at a fixed value of cycle/pixel and N is the total amount of spatial frequencies considered in the SFR (from 0 to 0.5 cycle/pixel).

Fig. 16 shows the SFR_σ values as a function of E2PR. The index is evaluated for each one of the tests of Table 1. As it happens for the discrepancy, when E2PR is below 0.1, the SFR_σ takes values always in the same range and

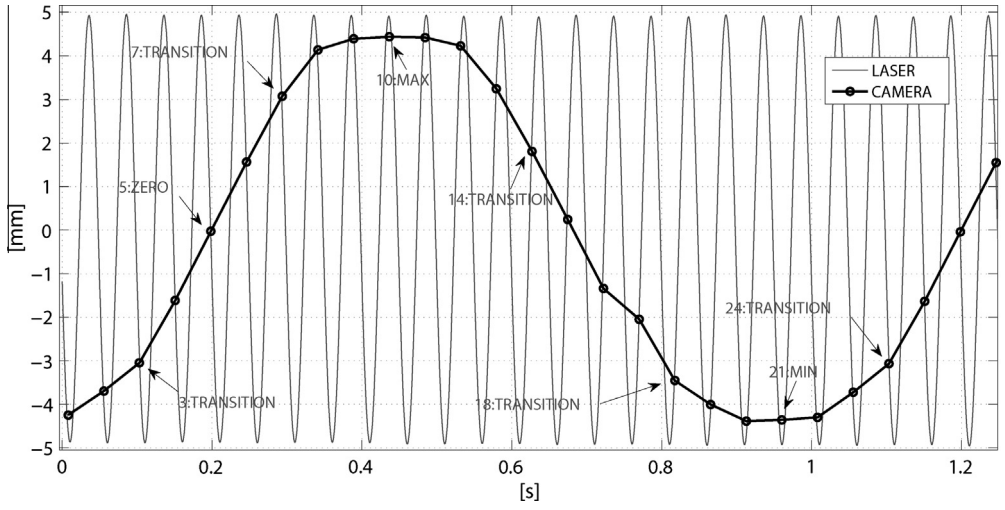

Fig. 13. Data measured in test conditions B: amplitude 5 mm, frequency 20 Hz, shutter 15 ms (camera in controlled aliasing).

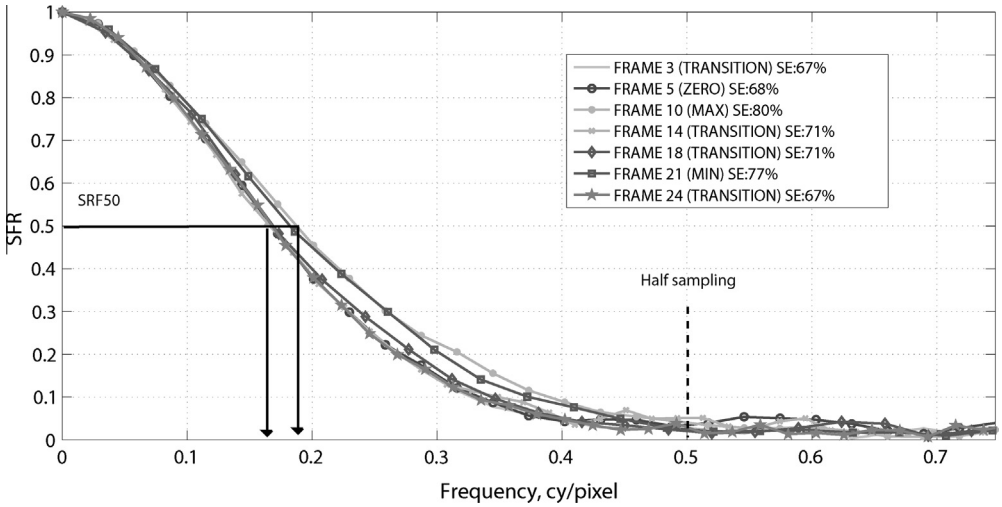

Fig. 14. SFR functions obtained in the test condition B.

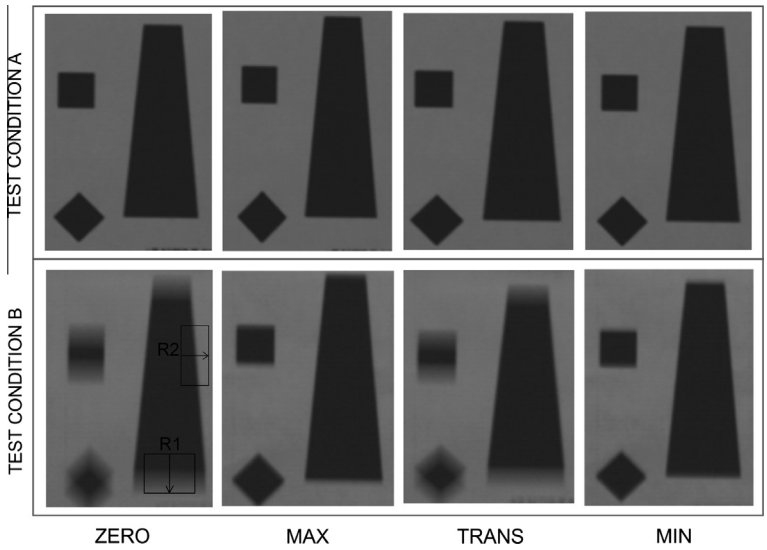

Fig. 15. Frames at positions zero, max, min, transition.

below 0.015. On the contrary, for E2PR values larger than 0.1, the SFR_σ shows an increasing trend, with a slope that strongly depends on the target vibration amplitude. However, in some cases, SFR_σ takes values below 0.015 even if the E2PR is upper to 0.1, especially when the target displacement is very low (i.e. $A \leqslant 3.5$ px).

It can be noticed that E2PR at 0.1 can be considered a threshold to discriminate static conditions only if the displacement amplitude is higher than 3.5 pixels. Fig. 17 indeed shows the percentage discrepancy (with respect to the imposed displacement) as a function of E2PR for all the data shown in Fig. 16 with a SFR_σ value below 0.015, which means their acquisitions should be considered almost static, relying on the SFR_σ parameter. When the displacement is $\leqslant$3.5 pixel, there are indeed SFR_σ values below 0.01, even in correspondence of tests where E2PR is higher than 0.1 (squared box in Fig. 17). This means that, even if the acquisition condition cannot be considered almost static, SFR_σ could have values below 0.015 when the amplitude displacement is too low. In conclusion, SFR_σ is a good estimator of the almost static acquisition conditions only when the displacement is >3.5 px, but it has the advantage of being based only on the quality of the image and no further information about the displacement are needed, since it is not necessary to know the grabbing frequency and the vibration frequency of the object, which are needed to estimate the E2PR value.

3.5.3. Blur influence

The purpose of this section is to evaluate the blur effect on the SFR_σ performances. Figs. 18 and 19 show a comparison among SFR_σ and discrepancy values obtained in different focus condition (good focus, moderate blurring,

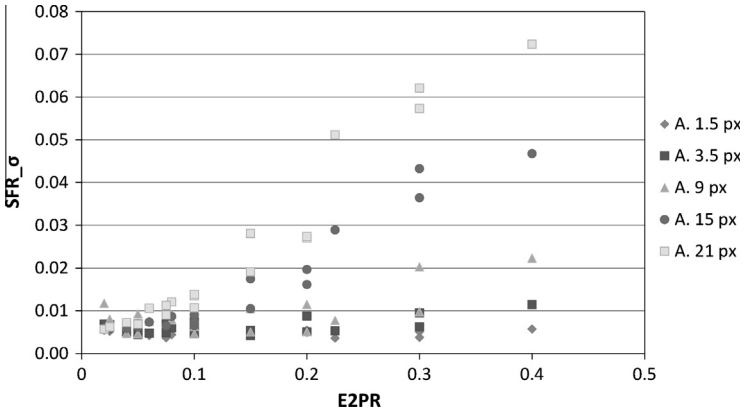

Fig. 16. SFR_σ values as function of E2PR value.

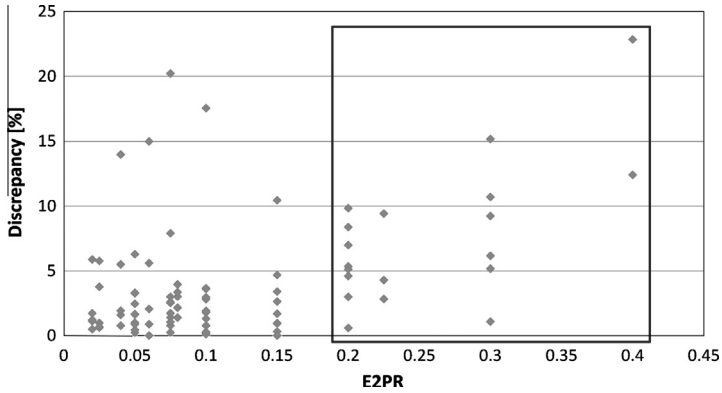

Fig. 17. Percentage discrepancy as function of E2PR value only for the data with SFR_σ around 0.01.

and strong blurring). As it was underlined in the Section 2, larger SFR values correspond to better focused images.

The results of Fig. 18 show that the discrepancy has similar trends for all the three defocusing levels. Defocusing seems indeed to be helpful in static condition (E2PR < 0.1), since the discrepancy takes lower values. This behavior is similar to that observed by Cantatore et al. [13] where the algorithm of edge detection shown improvement in case of defocused target.

In Fig. 19 the SFR_σ data show increasing values according to E2PR ratio when the image has a good focus, whereas the defocused tests present a lower increasing trend. Indeed, the gradient is as lower as the defocus is marked. This could be explained as the SFR_σ depends on the data variability but the image defocusing masks the dynamic effect and then the variability too. In the end, the SFR_σ is significant when the tests are performed in good focusing conditions.

3.6. Mean integral

It was underlined in the previous sections that larger values of the SFR curve correspond to higher image quality (see for example Fig. 2). Starting from this statement, another index based on SFR curves is proposed in addition to the SFR_σ index: the mean integral index (MI). The mean curve SFR is evaluated from all the SFR curves of the video (one curve for each frame), and then the integral underlying by the curve is estimated. The integral is calculated in the cycle/pixel range from 0 to 0.5, because for cycle/pixel larger than 0.5 the value of the curve tends to zero and only noise contribution is present.

The MI could reveal information about the whole quality of the test and if it is reliable or not. Fig. 20 shows the value of the mean integral as a function of the E2PR value obtained from the tests conditions summarized in Table 1.

The trend of the MI confirms that tests with exposure time lower than 10% of the target motion period (E2PR < 0.1) can be considered almost stationary. When E2PR is lower than 0.1, the mean integral is stable around the values 0.26 and 0.28, whereas for E2PR higher than 0.1 the mean integral increases linearly due to the dynamic which affects the image quality. This effect is much clearer when the displacement amplitude is high. However, the MI strongly depends on the image contrast and consequently it cannot be an absolute index. If an image of the fixed target is available, it is possible to estimate the MI in static condition and use this value as a reference for MI values during dynamic tests. If the MI in dynamic tests assumed values higher than the 90% of one estimated in the static case, the effect of the target dynamics on its displacement measurement is limited, whereas the effect of dynamics

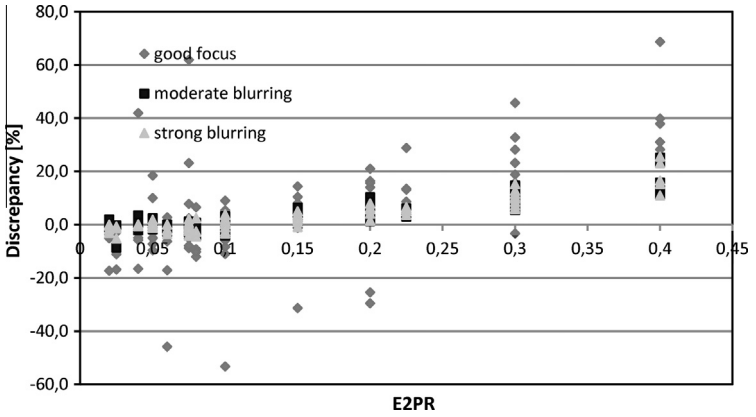

Fig. 18. Pixel discrepancy as function of E2PR for three blur levels.

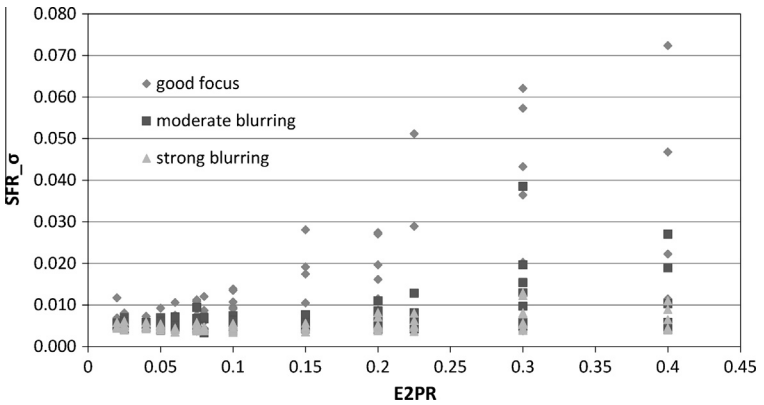

Fig. 19. SFR_σ as function of E2PR for three blur levels.

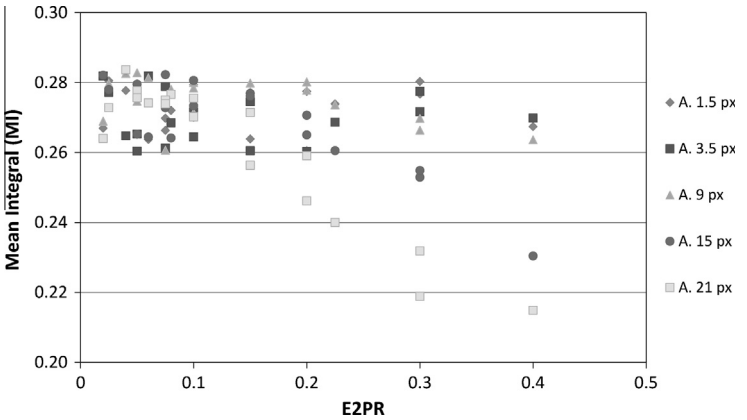

Fig. 20. MI values as function of E2PR.

becomes more and more important for the MI decrease under 90%.

4. Conclusion

Imaging devices used as displacement and vibration transducers are affected by measurement uncertainty as every common sensor. The uncertainty sources are difficult to quantify by a traditional calibration procedure, since camera performances are strictly linked to several parameters; some of them can be set before the acquisition, as diaphragm aperture and exposure time, but others depend on the environment conditions, like image contrast, and the target motion parameters.

In this work, a performance analysis of an imaging device applied to dynamic measurements is proposed. The analysis aims to qualify the measurement uncertainty by some indexes, proposed in this work and capable to estimate the effect of the target motion on the measuring results.

The E2PR index shows that the most important parameter for dynamic tests is the exposure time, because it impacts on the level of motion effect in the images. If the E2PR value is less than 0.1 the acquisition conditions can be considered almost-static and no appreciable motion blurring affects the acquired images.

The SFR_σ index allows qualifying the measurement uncertainty in the cases when no a priori information is available about the acquisition conditions. The index is obtained by the standard deviation of the SFR curves measured in correspondence of each clip frame. SFR_σ index is a good estimator of the almost static acquisition conditions only when the displacement are >3.5 px.

In the end, the MI index is proposed. It identifies a threshold value that confirms that the tests with exposure time lower than 10% of the target motion period can be considered almost stationary.

References

[1] Kostas Daniilidis, Petros Maragos, N. Paragios (Eds.), Computer Vision – ECCV 11th European Conference on Computer Vision, Springer, 2010.

[2] A. Hornberg (Ed.), Handbook of Machine Vision, John Wiley & Sons, 2007.

[3] A.N. Belbachi (Ed.), Smart Cameras, Springer, 2010.

[4] V. Tiwari, M.A. Sutton, S.R. McNeill, Assessment of high speed imaging systems for 2D and 3D deformation measurements: methodology development and validation, Exp. Mech. 47 (2007) 561–579.

[5] M.S. Kirugulige, H.V. Tippur, T.S. Denney, Measurement of transient deformations using digital image correlation method and high-speed photography: application to dynamic fracture, Appl. Opt. 46 (2007) 5083.

[6] W. Wang, J.E. Mottershead, C. Mares, Vibration mode shape recognition using image processing, J. Sound Vib. 326 (2009) 909–938.

[7] E. Zappa, P. Mazzoleni, A. Matinmanesh, Image Correlation Method in Dynamic Applications, accepted for publication in Optics and Laser in Engineering, Opt. Lasers Eng. 56 (2014) 140–151.

[8] S.W. Kim, N.S. Kim, Y.-M. Kim, Application of vision-based monitoring system to stay cables, in: F. Biondini, D.M. Frangopol (Eds.), Bridge Maintenance, Safety, Management, Resilience and Sustainability: Proceedings of the Sixth International IABMAS Conference, Stresa, Lake Maggiore, Italy, 8–12 July 2012, Taylor & Francis Ltd., 2012, pp. 1116–1123.

[9] G. Busca, A. Cigada, E. Zappa, Dynamic characterization of flexible structures through vision-based vibration measurements, Conf. Proc. Soc. Exp. Mech. Ser. 1 (2012) 189–196.

[10] S.W. Waterfall, J.H.G. Macdonald, N.J. McCormick, Targetless precision monitoring of road and rail bridges using video cameras, in: F. Biondini, D.M. Frangopol (Eds.), Bridge Maintenance, Safety, Management, Resilience and Sustainability: Proceedings of the Sixth International IABMAS Conference, Stresa, Lake Maggiore, Italy, 8–12 July 2012, Taylor & Francis Ltd., 2012, pp. 3976–3983.

[11] E. Caetano, S. Silva, J. Bateira, A vision system for vibration monitoring of civil engineering structures, Exp. Technol. 35 (2011) 74–82.

[12] E.S. Bell, J.T. Peddle, A. Goudreau, Bridge condition assessment using digital image correlation and structural modeling, Bridge Maintenance, Safety, Management, Resilience and Sustainability. In: Proceedings of the Sixth International IABMAS Conference, Stresa, Lake Maggiore, Italy, 8–12 July 2012, pp. 330–337.

[13] A. Cantatore, A. Cigada, R. Sala, E. Zappa, Hyperbolic tangent algorithm for periodic effect cancellation in sub-pixel resolution edge displacement measurement, Meas. J. Int. Meas. Conf. 42 (2009) 1226–1232.

[14] M. Shimizu, M. Okutomi, Sub-pixel estimation error cancellation on area-based matching, Int. J. Comput. Vis. 63 (2005) 207–224.

[15] ISO/TC: ISO 12233: Photography, Electronic still-picture cameras, Resolution measurements, ISO, 2000.

[16] P.D. Burns, Slanted-Edge MTF for Digital Camera and Scanner Analysis. Proc. PICS Conf., IS&T, 2000.

[17] M.A. Kriss, C.N. Nelson, F.C. Eisen, Modulation transfer function in photographic system containing development adjacency effects, Photogr. Sci. Eng. 18 (1974) 131–138.

[18] R.J. Polge, Digital computation of the modulation transfer function for arbitrary bar configurations, in: Proceedings – 15th Southeastern Symposium on System Theory, 1983, pp. 234–237.

[19] C. Gang, C. Xiaomei, N. Guoqiang, Performance estimation of optical system simulation based on MTF, in: Proceedings of SPIE – The International Society for Optical Engineering, 2009.

[20] D. Williams, Benchmarking of the ISO 12233 slanted-edge spatial frequency response plug-in, in: Society for Imaging Science and Technology: Image Processing, Image Quality, Image Capture, Systems Conference, 1998, pp. 133–136.

[21] M. Schulz, Measurement technique for the characterization of electronic still picture cameras, in: Proceedings of SPIE – The International Society for Optical Engineering, 1996, pp. 208–215.

[22] R. Bhaskar, J. Hite, D.E. Pitts, An iterative frequency-domain technique to reduce image degradation caused by lens defocus and linear motion blur, in: Proceedings of IGARSS'94 – 1994 IEEE International Geoscience and Remote Sensing Symposium, IEEE, 1994, pp. 2522–2524.